Electric Field Calculation on Residential Houses near UHVDC Lines Using 3D Reconstruction Method

Donglai Wang, Tiebing Lu, Xiang Cui, Li Xie, Luxing Zhao, Yong Ju, and Jiayu Lu

***Abstract*—Prediction of electric field on residential houses is required in the design of UHVDC transmission lines. The calculation of electric field distribution on houses is a 3D problem, however, the effectiveness of some 2D calculation methods has been validated by specific reduced-scale experimental models. The 2D methods are simple in operation and quick in computation compared with the 3D methods. In this paper, the deviation ranges of 2D electric field calculation results on the houses are discussed. Then, a 3D electric field reconstruction method is proposed to correct the 2D results according to the size and location of houses. The 3D electric field distribution on the house can be obtained based on 2D calculation efficiently, and the direct 3D calculation is avoided. Finally, the validity of the calculation methods are verified by the measurement results of a full-scale experimental system.**

***Index Terms*—3D reconstruction, corona discharge, electric field, residential house, UHVDC lines**

I. Introduction

CORONA discharge occurs near the surface of operating ultra-high voltage direct current (UHVDC) transmission lines. The ions generated by corona drift either toward the conductor of opposite polarity or toward the ground plane, and then strengthen the ground-level electric field, which is named as ion flow field problem [1-4]. The limit values of electric field strength under UHVDC lines are specified in the electromagnetic environment standards. However, due to the limitation of corridor width, the lines close to residential houses in China may be more common in the future with the construction of UHVDC projects. The presence of houses will distort the electric field near the house. Predicting the electric field on the houses near UHVDC lines accurately and efficiently is one of the important factors to design transmission lines, to determine house removal range and to settle disputes about electromagnetic environment.

This work was supported in part by the National Key Research and Development Program under Grant 2016YFB0900904 and in part by the Science and Technology Project of State Grid Corporation of China GYB17201400185.

D. Wang T. Lu and X. Cui are with the State Key Laboratory of Alternate Electrical Power System with Renewable Energy Sources, North China Electric Power University, Beijing 102206, China (e-mail: donglaiwang@ncepu.edu.cn;).

L. Xie, L. Zhao, Y. Ju and J. Lu are with the China Electric Power Research Institute, Beijing 100192, China.

In the past decades, many scholars have made important contributions on the improvement of electric field and ion current calculation strategies, and a variety of methods have been proposed [5-8]. The methods for ground-level electric field calculation with houses nearby can be divided into 2D methods and 3D methods. In 2D methods, the length of houses in the direction that parallel to the lines is considered to be infinite. In 2010, 2D flux tracing method (FTM) was proposed by Luo et al to calculate the ground-level electric field with houses nearby [9]. In FTM, the Deutsch assumption is used to simplify the calculation. Then, Zhen et al. and Huang et al. abandoned Deutsch assumption and presented a 2D optimized finite element method (FEM), respectively [10, 11]. Zhen et al. also studied the influence of the electrical conductivity of house on electric field strength by 2D FEM [12].

2D methods are more achievable in engineering practice for their simple operation. But essentially, the electric field distribution near the house is a 3D problem, 2D methods always have certain errors and cannot provide the electric field variation in the dimension that parallel to the lines. Therefore, Luo et al. extended the FTM to the 3D situation [13]. Li et al. calculated the electric field on a human body based on the 3D FTM [14], and Zhou et al. calculated the shielding effect of 3D wire mesh under HVDC transmission lines based on the same theory [15]. The mesh-based methods, such as FEM, are not fit for dealing with open domain problems, because excessive computation resources are required. So the hybrid 2D/3D method was put forward to reduce the computation scale [16-18]. In hybrid 2D/3D method, the influence of house is limited to its surroundings, so the 2D calculation result at a distance from the houses can be used as the boundary conditions of the 3D calculation domain near the houses. Thus, 3D calculation is confined in a smaller area. Because of the limitation of computation cost, direct 3D mesh-based methods only used in the calculation of a reduced-scale house model [19], or the bundle conductors in the calculation model are simplified to equivalent single conductors [20, 21].

In conclusion, both 2D and 3D methods have their own advantages in ion flow field calculation, but the differences between 2D and 3D methods are still subjected to be investigated. Besides, all the proposed ion flow field calculation methods on houses have not been verified by full-scale experimental models until now. In order to complete a large number of UHVDC line design work efficiently, it is

significant to determine the effective range of 2D calculation methods.

In this paper, the difference of 2D and 3D calculation results around the houses is presented, and the deviation range of the 2D and 3D methods is given. To make full use of the advantages of 2D methods, a 3D electric field reconstruction method is proposed to correct the 2D calculation results. In the 3D reconstruction method, 3D electric field distribution on the house can be obtained almost without additional calculating time compared with corresponding 2D method. Relying on the UHVDC Test Base of China Electric Power Research Institute, a full-scale electric field experimental system with houses nearby is built. The engineering practical effectiveness of 3D Deutsch assumption-based electric field calculation method as well as the 3D reconstruction method are testified by the experiment.

II. Analysis Model with Houses

The diagram of the analysis model that a flat roof house near bipolar UHVDC lines is shown in Fig. 1. The house is simplified as a cuboid. Two sides of the house are vertical to the lines and other sides are parallel to it. In Fig. 1, a rectangular coordinate system xyz is established on the ground. D is the distance between positive and negative polar lines; H is the height of lines. The centre of house is located on x=0. D_h is the minimum distance from the centre of lines to the edge of house; L_h, W_h and H_h are the length, width and height of the house, respectively. To reflect the electric field distribution characteristics around the house concisely, three paths, marked as Path I (x=0), Path II (x=0.4L_h) and Path III (x=L_h/2+H_h/2), respectively, are selected to be the specific calculation paths in 3D calculation. When the paths across the house, the electric field on the roof is considered. Otherwise, the ground-level electric field is calculated. P_I, P_{II} and P_{III} are intersection points of the centreline of house (y=D_h+W_h/2) and the paths.

The governing equations for the ion flow field in calculation region are given as follows:

$$\nabla \cdot \boldsymbol{E} = \left(\rho_+ - \rho_-\right)/\varepsilon_0 \tag{1}$$

$$\begin{cases} \nabla \cdot \left(\rho_+ \mu_+ \boldsymbol{E}\right) = -R\rho_+\rho_-/e \\ \nabla \cdot \left(\rho_- \mu_- \boldsymbol{E}\right) = R\rho_+\rho_-/e \end{cases} \tag{2}$$

where $\boldsymbol{E}$, φ are the electric field vector and potential in the ion flow field, respectively, $\boldsymbol{J}$ is the ion current density, μ is the ion mobility rate, R is the ion recombination coefficient, e is the charge of the electron, ρ is the space charge density (non-negative value), ε_0 is the permittivity in the air,. The subscript "+" is for positive and "-" is for negative.

The boundary conditions are defined as follows [12]:

$$\begin{aligned} &\varphi\big|_{\Gamma_1} = U \\ &\varphi\big|_{\Gamma_2} = 0 \\ &\left.\frac{\partial \varphi}{\partial n}\right|_{\Gamma_1} = E_{on} \end{aligned} \tag{3}$$

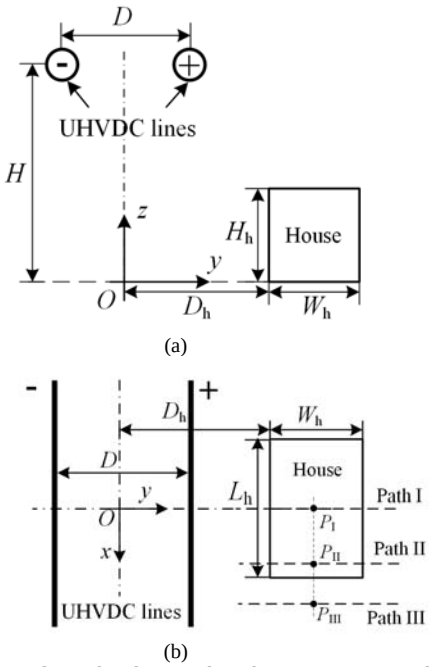

Fig. 1. The position relationship diagram that a house near UHVDC lines. (a) Front view. (b) Plan view

where U, E_{on} are the voltage and corona onset electric field of transmission lines, respectively, Γ_1 is the surface of lines, Γ_2 is the surface of ground and houses. The corona onset electric field E_{on} can be obtained by Peek's law in DC form [22].

To simplify the calculation, Deutsch assumption, i.e., the space charges only affect the magnitude of the electric field without changing its direction, is adopted. The influence of towers and the sag of transmission lines are neglected, and the houses are considered as perfect conductors [12].

Based on Deutsch assumption, the ground-level electric field and space charge density can be obtained by the integral along with the electric flux line. And the space-charge-free electric field is calculated by charge simulation method. 2D and 3D methods are used to calculate the electric field around the house, respectively. Infinite length line charges are put into the lines and the house in 2D method. In the 3D method, the simulation charges in the house are replaced by point charges.

III. Comparison Between 2D and 3D Methods

A. Difference of 2D and 3D calculation results

The parameters of two different UHVDC line structures are listed in Table I. The voltages are ±800kV and ±1100kV, respectively. The difference of 2D and 3D methods depends on the size and location of house. As an example, the parameters of the house in Fig. 1 are set as L_h=12m, W_h=6m, H_h=4m, D_h=30m. The voltages on the lines are ±800kV.

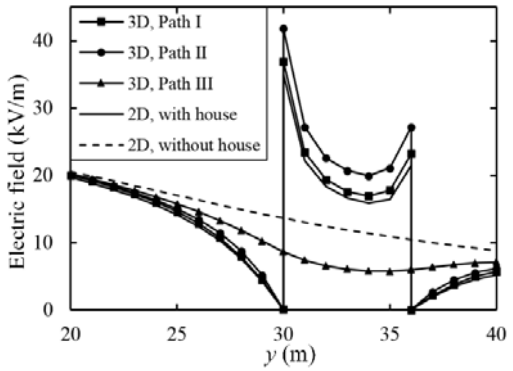

Fig. 2. Electric field distributions calculated by 2D and 3D methods

TABLE I
PARAMETERS OF THE UHVDC TRANSMISSION LINES

Parameters	±800kV	±1100kV
Conductor type	6×720mm^2	8×1000mm^2
Bundle spacing	45cm	40cm
Height	19m	26m
Polar distance	22m	26m

The 2D and 3D electric field calculation results under different circumstances are shown in Fig. 2. The existence of house has a shielding effect on the electric field on the ground near the house. The field strength on the roof is much higher than ground, especially at the corner area of the roof. When dealing with the ground-level electric field at the front or rear area of house, in other words, $y \leqslant D_h$ or $y \geqslant D_h+W_h$, the results from the 2D and 3D methods are almost the same. On the roof, 2D and 3D field distribution curves have almost the same shape. 2D results may approach to 3D on Path I, but significantly less than 3D on Path II. Furthermore, the results from 2D method can hardly reflect the ground-level electric field distribution at the side area of the house, such as on Path III.

B. Deviation range of 2D methods

Because of the limitation of construction period or technological level, in some cases, only 2D calculation methods are available for engineers. It is important to estimate the deviation range and relative error of 2D methods. The relative error of 2D and 3D methods depends on the geometric parameter of houses. Based on the calculation model in *Section III. A*, the method of control variables is applied to study the influence of parameter L_h, W_h, H_h and D_h on 2D and 3D calculation results. P_0 is a point in 2D space. The y and z coordinate of P_0 has the same value with P_I and P_{II} in 3D space. In other words, $P_I(x, y, z) = (0, D_h+W_h/2, H_h)$, then $P_0(y, z) = (D_h+W_h/2, H_h)$. Besides, in the next, when W_h is considered as the independent variable, $P_I(x, y, z)$ is kept at point $(0, D_h+3, H_h)$.

Comparisons between 2D and 3D calculation results are shown in Fig. 3. Results from 3D method are always larger than those from 2D method on the roof. The electric field strength on P_I is the closest value to that on P_0. The difference between field strength on P_I, P_{II} and P_0 shrinks with the increase of L_h, D_h, and with the decrease of W_h, H_h. Besides, L_h and H_h are two of the most significant variables that affect the difference of 2D

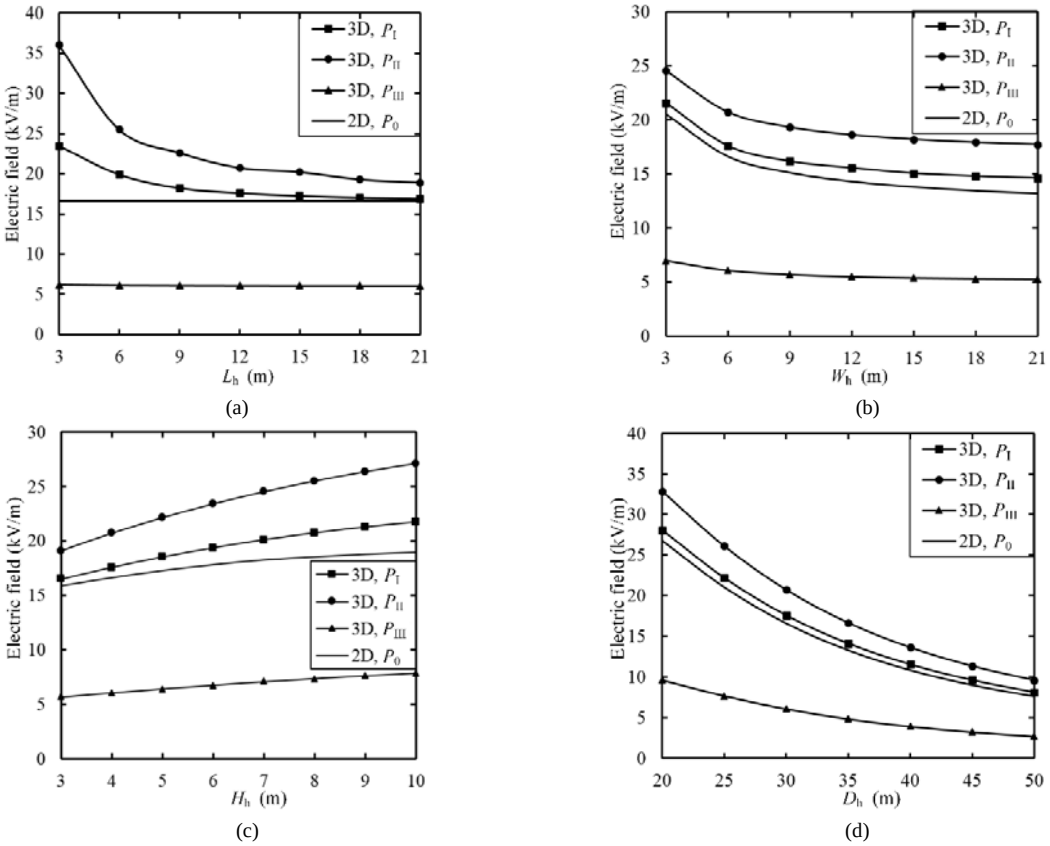

Fig. 3. Influence of house model parameters on 2D and 3D calculation results. (a) Varies of L_h. (b) Varies of W_h. (c) Varies of H_h. (d) Varies of D_h.

and 3D calculation results.

IV. 3D Electric Field Reconstruction Method

A. Calculation area division and sample selection

Although there are some limitations in the 2D methods, however, the influence of conductor structures, corona discharge status and part of the ground-level electric field distribution information can be obtained by 2D calculation. To extend the applicable range of 2D methods, a method that reconstruct 3D electric field distribution on the house according to 2D results is presented.

According to the conclusions from the comparison of 2D and 3D calculation results, the area around the house can be divided into three parts, as shown in Fig. 4. Area 1 is the roof of house, i.e., $x \in (-L_h/2,\ L_h/2)$ and $y \in (D_h,\ D_h+W_h)$, $z=H_h$. Area 3 is $x \geqslant L_h/2$, $z=0$. The rest area on the ground is Area 2.

In Area 2, 2D calculation results are almost equal to 3D results. In Area 1, the2D and 3D electric field distribution curve on the direction perpendicular to lines have similar shapes. In Area 3, the house always has a shielding effect on the electric field around itself, so the upper limit of electric field in this area can be determined by 2D methods considering the absence of house. The field strength under the wall is zero. Above all, 3D electric field distribution around the house can be reconstructed from 2D as follows:

$$E_{3D}(x,y)=\begin{cases}\left[1+k(x)\right]\cdot E_{2D}(y) & (\text{in Area 1})\\ E_{2D}(y) & (\text{in Area 2})\\ f\left[E_{2D}(y),E_a(y),x\right] & (\text{in Area 3})\end{cases} \quad (4)$$

where x and y present the coordinate of points on the ground and roof, k and f are the scalar functions, $E_{3D}(x, y)$ is the reconstructed 3D electric field distribution around the house, $E_{2D}(y)$ is the 2D calculation result with the existence of house, and $E_a(y)$ is the 2D results with the absence of house. For each specific calculation sample, the parameters of lines and house structures are regarded as constant values.

In equation (4), if the function k and f can be determined according to 2D calculation results and the geometric parameter of houses, the ground-level electric field prediction in the whole area around the house will no further rely on direct 3D calculation. To summarize this relationship, the cubic house models with 3360 different parameters are selected as the samples. The ranges of house parameters are listed in Table II. The voltage on the lines is ±800kV.

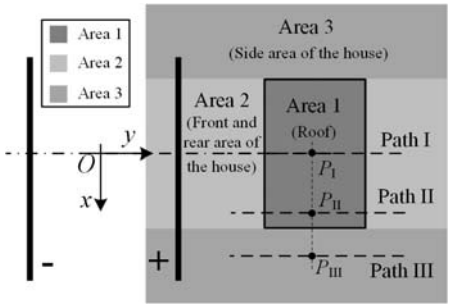

Fig. 4. Area division diagram

B. 3D Reconstruction Formula in Area 1

The most important step of 3D electric field reconstruction in Area 1 is determining the function $k(x)$. To make the consequence more general, $k(x)$ is defined as:

$$k(x)=k\big|_{y=y_0}(x)=\frac{E_{3D}(x,y_0)-E_{2D}(y_0)}{E_{2D}(y_0)} \quad (5)$$

where $y_0=D_h+W_h/3$. Then, curve fitting method is used to discuss the relationship between $k(x)$ and L_h, W_h, H_h, D_h. Among all the independent variables, L_h is the most significant factor that affects the value of $k(x)$. So the influence of L_h is discussed separately. Under each given W_h, H_h, D_h, the value of $k(x)$ on Path I and Path II, noted as k_I and k_{II}, can be obtained not only from the direct 2D and 3D calculation by (5), but also from specific fitting equation, as shown below:

$$\begin{cases}k_I=a_I\exp(-b_I L_h)+c_I\\ k_{II}=a_{II}\exp(-b_{II}L_h)+c_{II}\end{cases} \quad (6)$$

where a_I, b_I, c_I, a_{II}, b_{II}, c_{II} are the fitting coefficients related to W_h, H_h, D_h. In each combination of W_h, H_h, D_h, (6) has its specific fitting coefficients. Let W_h=6m, H_h=7m, D_h=30m, in this case, a_I=1.09, b_I=0.28, c_I=0.05, a_{II}=2.94, b_{II}=0.31, c_{II}=0.23, the fitting result of k_I, k_{II} and L_h is shown in Fig. 5. It turns out to be that the exponential function form like (6) fits the relationship of k_I, k_{II} and L_h well.

Next, multiple regression analysis is used to calculate the fitting relationship between W_h, H_h, D_h and the coefficients a_I, b_I, c_I, a_{II}, b_{II}, c_{II} in (6). The flow chart of this step is shown in Fig. 6, and the result can be written as:

$$\boldsymbol{B}_1=\mathbf{A}_1\boldsymbol{X}_1 \quad (7)$$

TABLE II
Size and Location of the House Models

	Minimum (m)	Maximum (m)	Interval (m)	Sample quantity
Length (L_h)	3	30	3	10
Width (W_h)	3	18	3	6
Height (H_h)	3	10	1	8
Distance (D_h)	20	50	5	7
Total				3360

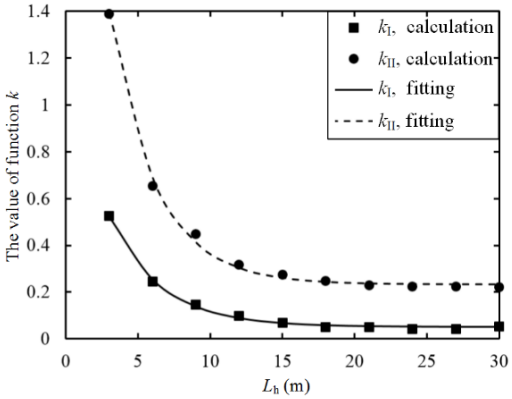

Fig. 5. The effect of exponential function fitting when k_I, k_{II} varies with respect to L_h.

where $\boldsymbol{B}_1 = [a_1, b_1, c_1, a_{II}, b_{II}, c_{II}]^T$

$\boldsymbol{X}_1 = [1, W_h, H_h, D_h]^T$

$$\mathbf{A}_1 = 10^{-3} \times \begin{bmatrix} 184.1 & 35.3 & 82.5 & 3.0 \\ 329.6 & -1.2 & -5.0 & -0.3 \\ -34.8 & 1.9 & 9.0 & 0.5 \\ 1183.4 & 45.0 & 183.9 & 6.2 \\ 347.3 & -2.2 & -1.9 & -0.1 \\ -11.9 & 7.9 & 24.1 & 1.0 \end{bmatrix}$$

Matrix $\mathbf{A}_1$ is a constant matrix that can be applied in various line structures and voltages, for the influence of these factors are included in 2D calculation results.

The value of $k(x)$ for each x on the roof is:

$$k(x) = k_I + (k_{II} - k_I)\left(\frac{x}{0.4L_h}\right)^2 \tag{8}$$

where $x \in [0, L_h/2)$. After obtaining the parameters in matrix $\mathbf{A}_1$, the curve fitting method is not required in the 3D reconstructed calculation any more, and the direct 3D calculation is also avoided. In the practical application, the 3D electric field on Area 1 can be reconstructed by performing the simple algebraic operations according to the equation (7), (6), (8) and (4) successively.

C. 3D Reconstruction Formula in Area 3

The transformation relation of 2D and 3D calculation results in Area 3 is represented by the scalar function f. The electric field distribution regularity on the direction perpendicular to lines in this area cannot be obtained directly just like that in Area 1. Therefore, the electric field on Path III is selected to describe the shielding degree of house at first. The function $s(y)$, named as shielding factor, is defined as:

$$s(y) = \frac{E_a(y) - E_{III}(y)}{E_a(y)} = a_{III} \exp\left[-b_{III}(y_s - c_{III})^2\right] \tag{9}$$

where $y_s = (|y| - D_h)/W_h - 1/2$, $E_{III}(y)$ is the electric field on Path III. In (9), when a_{III}=0.53, b_{III}=1.06 and c_{III}=0.05, the comparison between direct 2D and 3D calculation and exponential fitting results of $s(y)$ is shown in Fig. 7. The result indicates that the former direct 2D and 3D calculation in (9) can be replaced by the later fitting equation.

The coefficients a_{III}, b_{III} and c_{III} are also calculated by multiple regression analysis according to Fig. 6. The fitting result can be written as:

$$\boldsymbol{B}_3 = \mathbf{A}_3 \boldsymbol{X}_3 \tag{10}$$

where $\boldsymbol{B}_3 = [a_{III}, b_{III}, c_{III}]^T$

$\boldsymbol{X}_3 = [1, W_h, H_h, W_h^2]^T$

$$\mathbf{A}_3 = 10^{-3} \times \begin{bmatrix} 421.0 & 33.3 & -22.6 & -1.1 \\ 427.2 & 161.0 & -87.5 & -5.3 \\ 51.0 & -16.0 & 19.5 & 0.7 \end{bmatrix}$$

$\mathbf{A}_3$ is also a constant matrix that can be applied in different line structures and voltages. The electric field on Path III is calculated by:

$$E_{III}(y) = [1 - s(y)] E_a(y) \tag{11}$$

The 3D reconstructed equation on Area 3 is presented as follow:

$$\begin{aligned} E_{3D}(x, y) &= f[E_{2D}(y), E_a(y), x] \\ &= E_a(y) - [E_a(y) - E_{2D}(y)] \\ &\quad \cdot \left[\frac{E_a(y) - E_{III}(y)}{E_a(y) - E_{2D}(y)}\right]^{\frac{2}{H_h}\left(x - \frac{L_h}{2}\right)} \end{aligned} \tag{12}$$

Above all, the 3D reconstruction work in Area 3 is calculating (10), (9), (11) and (12) successively according to 2D results and the structure of house.

When dealing with a 12m×6m×4m house, in direct 3D calculation method, 1382 simulation charges are put in the house model, and electric field calculation time of 100 points on the ground is 337.7 seconds. However, in 2D calculation, the number of simulation charges in the house is 54, and the time cost is 4.2 seconds. In addition, the time cost of 3D reconstruction work is less than 0.01 second.

V. Verification of Calculation Methods

A. Experimental setup

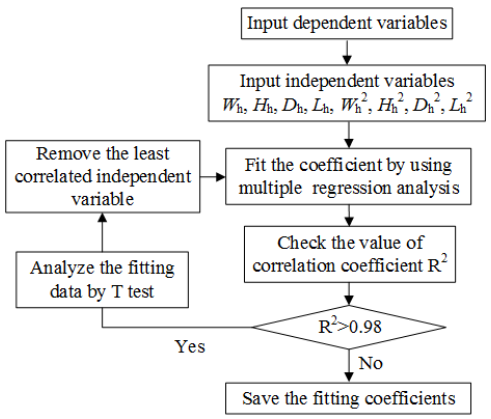

Fig. 6. Flow chart of multiple regression analysis.

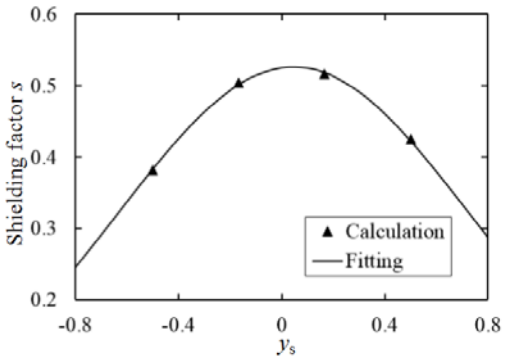

Fig. 7. Fitting effect of shielding factor $s(y)$ on Path III

To testify the different calculation methods utilized and proposed in this paper, a full-scale test site is established, as shown in Fig. 8(a). The test span is located in the middle of the whole test transmission lines, and the length of which is 300m.

The voltage of DC source is adjustable, and the maximum output voltage is ±1200kV. Two houses with the same size are put symmetrical about the centre of the transmission lines. The material of houses are brick-concrete composite structure. D_h, L_h, W_h and H_h are 30m, 12m, 6m and 4m, respectively.

The field mills, as shown in Fig. 8(b), are used to measure electric field. Measurement data with relative humidity of 50%-70% are recorded, and the average values of measurement results are taken as the actual ground-level electric field strength.

B. Validity of electric field calculation

In the experiment, the voltages applied on the transmission lines are ±800kV and ±1100kV, respectively. Both the 3D Deutsch assumption-based method and the 3D reconstruction method are used to calculate the distribution of electric field around the house.

Comparisons between measurement and calculation results are shown in Fig. 9 and Fig. 10. Measurement results, the results from the direct 3D calculation method and those from the 3D reconstruction method are indicated by points, solid lines and dotted lines, respectively. Electric fields under ±800kV lines are shown in Fig. 9(a) and Fig. 9(b), respectively. Electric fields under ±1100kV lines are shown in Fig. 10(a) and Fig. 10(b), respectively. Electric field distribution at the positive and negative side of transmission lines are shown by the colour of red and blue, respectively.

Because of the complexity of corona discharge effect and the impact of environment, the randomness of measurement results with large-scale transmission lines are always strong [1, 11, 22]. The electric field measurement probes are calibrated by parallel plate electrodes. When the probes are put on the roof or the ground that adjacent to the wall, the edges of house may also impact the precision of the measurement results. In general, the calculation and measurement results are in good agreement, especially on the ground. As for the electric field on the roof, 3D reconstruction results are almost the same with the direct 3D calculation in the centre area, but smaller at the marginal area of roof.

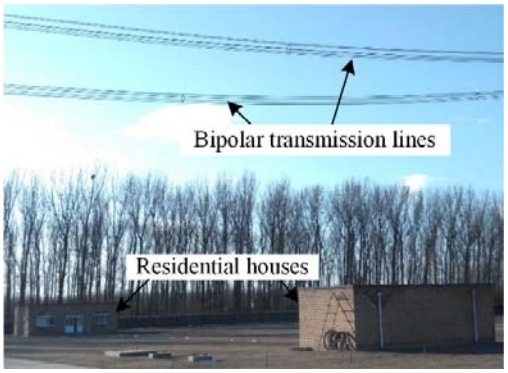

(a)

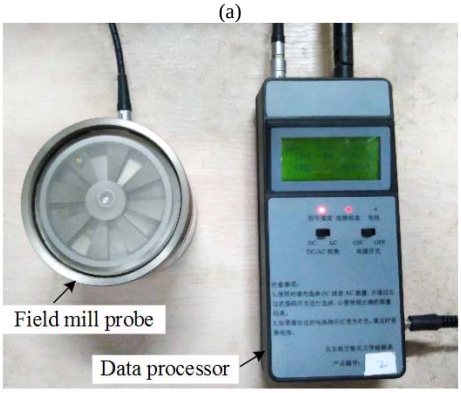

(b)

Fig. 8. Full-scale experiment. (a) Transmission lines and houses. (b) Electric field measuring equipment.

The parameters in 3D reconstruction method are extracted according to the ±800kV lines. To verify the generality of this method, electric field on the whole 3360 model house structures under ±1100kV lines are calculated as well. The values of k_I, k_{II} and E_{III} from both direct 3D calculation and 3D reconstruction method are compared. The maximum relative error is 7.4%. Besides, in Fig. 10, the shapes of solid and dotted electric field distribution curves also reflect the good consistency of the two methods. Therefore, 3D reconstruction method has wide applications.

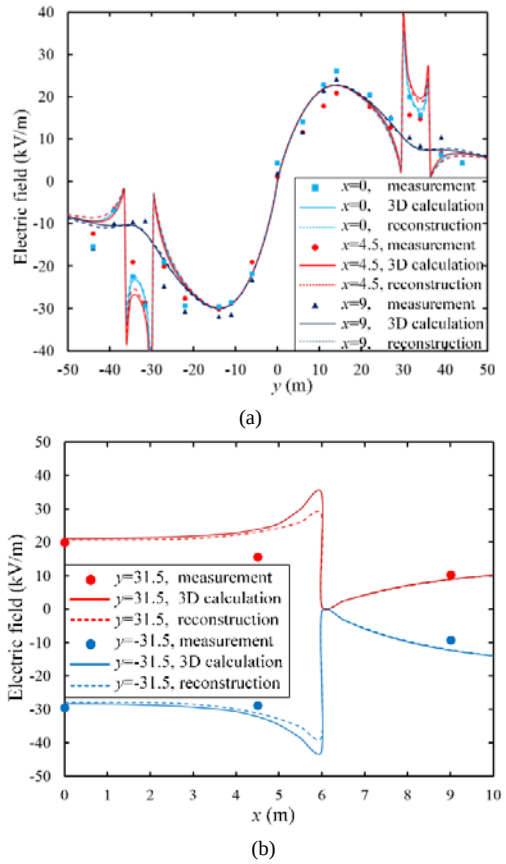

Fig. 9. Verification of calculation methods under ±800kV lines. (a) Calculation paths perpendicular to the lines. (b) Calculation paths parallel to the lines.

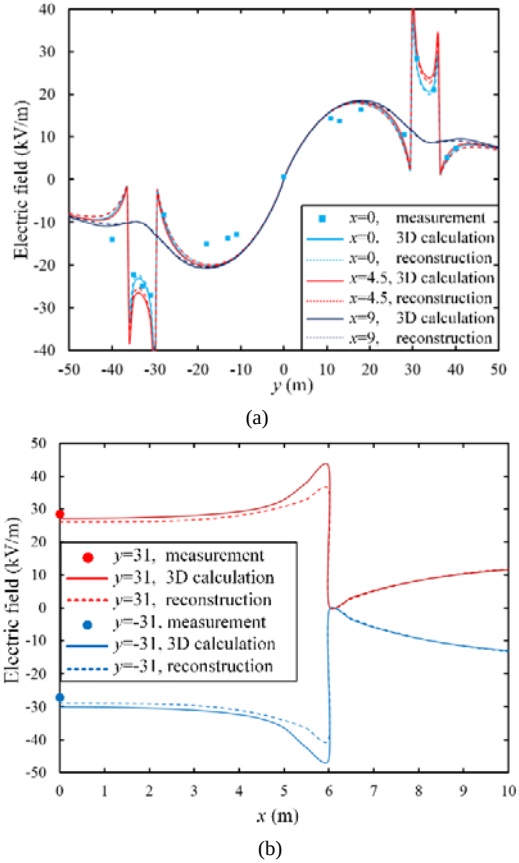

Fig. 10. Verification of calculation methods under ±1100kV lines. (a) Calculation paths perpendicular to the lines. (b) Calculation paths parallel to the lines.

The global ground-level electric fields around the house calculated by direct 3D method and 3D reconstruction method near ±800kV lines are shown in Fig. 11(a) and Fig. 11(b), respectively. The 3D reconstruction method can reflect the shielding effect of the house precisely. Meanwhile, the reconstructed electric field strength on the roof can also satisfy the practical demand in engineering.

VI. Conclusions

The difference between 2D and 3D space charge electric field calculation method under UHVDC lines with houses nearby is discussed. A 3D electric field reconstruction method is proposed to make full use of the simple and efficient characteristics of 2D methods. The following conclusions may be drawn:

1） 2D calculation methods are simple and effective, but they cannot reflect the 3D electric field distribution around the house directly. 3D calculation results on the roof that perpendicular to the transmission lines are always larger than 2D results. However, the difference shrinks with the increase of the length of house, and decrease of width, height of house as well as the distance between transmission lines and the house.

2） 3D electric field distribution is reconstructed from 2D calculation results according to the geometry structure of houses by four steps of algebraic operation. The time cost

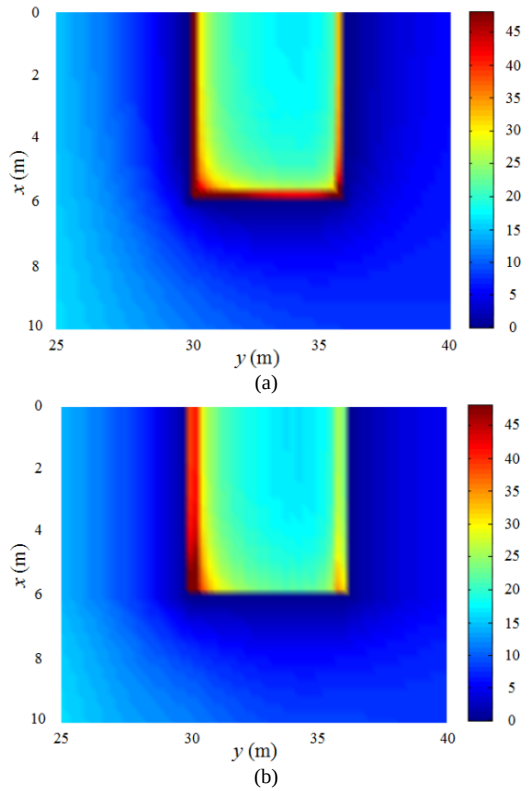

Fig. 11. Global electric field distribution near ±800kV lines (kV/m). (a) Direct 3D calculation. (b) 3D reconstruction method

of 3D reconstruction work is less than 0.01 second when dealing with a common house model. Therefore, the efficiency of 3D electric field distribution analysis around the house is improved obviously.

3） A full-scale experimental system is built to measure the electric field. The validity of calculation methods in this paper are verified by the measurement data. 3D Deutsch assumption-based calculation results are consistent with the experiment under the voltage of both ±800kV and ±1100kV. Electric field calculated by 3D reconstruction method agreed well with direct 3D calculation on the ground and centre area of roof, but smaller at the marginal area of roof.

REFERENCES

[1] P. S. Maruvada, “Influence of Ambient Electric Field on the Corona Performance of HVdc Transmission Lines,” IEEE Trans. Power Deli., vol. 29, no. 2, pp. 691-698, Apr. 2014.

[2] P. S. Maruvada and W. Janischewskyj, “Analysis of Corona Losses on DC Transmission Lines Part I - Unipolar Lines,” IEEE Trans. Power App. Syst., vol. PAS-88, no. 5, pp. 718-730, May 1969.

[3] Z. Zou, X. Cui, T. Lu, “Analysis of dielectric particles charging and motion in the direct current ionized field,” CSEE J. Power and Energy Syst., vol. 2, no. 1, pp. 88-94, Mar. 2016.

[4] Z. Wang, T. Lu, X. Cui, X. Li and H. Hiziroglu, “Influence of AC voltage on the positive DC corona current pulses in a wire-cylinder gap”, CSEE J. Power and Energy Syst., vol. 2, no. 4, pp. 58-65, Dec. 2016.

[5] W. Janischewskyj and G. Cela, “Finite Element Solution for Electric Fields of Coronating DC Transmission Lines,” IEEE Trans. Power App. Syst., vol. PAS-98, no. 3, pp. 1000-1012, May 1979.

[6] T. Takuma and T. Kawamoto, “A Very Stable Calculation Method for Ion Flow Field of HVDC Transmission Lines,” IEEE Trans. Power Deli., vol. 2, no. 1, pp. 189-198, Jan. 1987.

[7] Z. M. Al-Hamouz, “Corona power loss, electric field, and current density profiles in bundled horizontal and vertical bipolar conductors,” IEEE Trans. Ind. App., vol. 38, no. 5, pp. 1182-1189, Sep./Oct. 2002.

[8] J. Qiao, J. Zou and B. Li, “Calculation of the ionised field and the corona losses of high-voltage direct current transmission lines using a finite-difference-based flux tracing method,” IET Gene., Trans. & Distrib., vol. 9, no. 4, pp. 348-357, Mar. 2015.

[9] Z. Luo et al., “Calculation method for the ionized field under HVDC transmission line with building nearby,” (in Chinese) Proceedings of the CSEE, vol. 30, no. 15, pp. 125-130, May 2010.

[10] Y. Zhen et al., “Finite element method for calculating total electric field of HVDC lines with underneath building,” (in Chinese) Proceedings of the CSEE, vol. 31, no. 9, pp. 120-125, Mar. 2011.

[11] G. Huang et al., “Calculation of the ionized field under DC transmission lines with buildings nearby,” (in Chinese) Proceedings of the CSEE, vol. 32, no. 4, pp. 193-198, Feb. 2012.

[12] Y. Zhen et al., “Ion Flow Field Analysis Considering the Finite Conductivity of the Building Near HVDC Transmission Lines,” IEEE Trans. Magn., vol. 51, no. 3, pp. 1-4, Mar. 2015.

[13] Z. Luo, X. Cui, W. Zhang and J. Lu, “Calculation of the 3D Ionized Field Under HVDC Transmission Lines,” IEEE Trans. Magn., vol. 47, no. 5, pp. 1406-1409, May 2011.

[14] X. Li et al., “The Ionized Fields and the Ion Current on a Human Model Under ±800-kV HVDC Transmission Lines,” IEEE Trans. Power Deli., vol. 27, no. 4, pp. 2141-2149, Oct. 2012.

[15] X. Zhou, T. Lu, X. Cui and Y. Zhen, “Analysis of the Shielding Effect of Wire Mesh to Ion Flow Field From HVDC Transmission Lines,” IEEE Trans. Magn., vol. 50, no. 2, pp. 89-92, Feb. 2014.

[16] B. Zhang, W. Li, J. He and R. Zeng, “2D/3D hybrid computation of ion flow field around house near HVDC bipolar transmission lines,” in 14th IEEE Conf. Elect. Field Comp. (CEFC), Chicago, IL, 2010, pp. 1-1.

[17] Y. Zhen, X. Cui, T. Lu, X. Li, C. Fang and X. Zhou, “3D Finite-Element Method for Calculating the Ionized field and the Ion Current of the Human Body Model Under the UHVDC Lines,” IEEE Trans. Power Deli., vol. 28, no. 2, pp. 965-971, Apr. 2013.

[18] B. Zhang, H. Yin, J. He and R. Zeng, “Computation of Ion-Flow Field Near the Metal Board House Under the HVDC Bipolar Transmission Line,” IEEE Trans. Power Deli., vol. 28, no. 2, pp. 1233-1234, Apr. 2013.

[19] G. Huang et al., “Improved 3D upwind FEM for solving ionized field of HVDC transmission lines,” Proceedings of the CSEE, vol. 33, no. 33, pp. 152-159, Nov. 2013.

[20] Y. Zhen, X. Cui and T. Lu, “Modeling of an ionized field on the building near the UHVDC transmission lines,” Science China Technological Sciences. Vol. 57, no. 4, pp. 747-753, Apr. 2014.

[21] X. Zhou, T. Lu, X. Cui, Y. Liu and X. Li, “Simulation of Ion-Flow Field at the Crossing of HVDC and HVAC Transmission Lines,” IEEE Trans. Power Deli., vol. 27, no. 4, pp. 2382-2389, Oct. 2012.

[22] Y. Yang, J. Lu and Y. Lei, “A Calculation Method for the Electric Field Under Double-Circuit HVDC Transmission Lines,” IEEE Trans. Power Deli., vol. 23, no. 4, pp. 1736-1742, Oct. 2008.